scientific reports

Check for updates

OPEN

Enhanced HGF with increased receptor affinity and nitration-dysfunction resistance through interaction with lipoic acid trisulfide

Kahona Zushi[1,7], Miyumi Seki[1,7], Ryota Mizuochi[1], Kazuki Shitamitsu[1], Alaa Elgaabari[1,2], Sakiho Tanaka[1], Junri Miyamoto[1], Kaoru Mizoguchi[1], Reina Fujimaru[1], Jiaxi Han[1], Takashi Nakashima[3], Shoko Sawano[4], Wataru Mizunoya[5], Takahiro Maeno[1], Issei Yokoyama[1], Takahiro Suzuki[1], Judy E. Anderson[6] & Ryuichi Tatsumi[1]✉

Myogenic stem cell activator HGF (hepatocyte growth factor) undergoes nitration of tyrosine residues (Y198, Y250) predominantly on fast-twitch fibers to lose its binding affinity to the signaling receptor c-met, in response to peroxynitrite ($ONOO^-$) generation during aging. Here we show that HGF adopts an enhanced form with dynamically increased receptor-binding affinity and nitration-dysfunction resistance through interaction with lipoic acid trisulfide (LASSS) under physiological conditions. When evaluated after exposure to LASSS at a 1:8000 molar ratio to HGF and subsequent ultra-filtration to wash-out un-reacted free LASSS, c-met binding affinity increased more than two-fold over the original non-nitrated HGF. The same LASSS treatment also conferred nitration resistance with a greater effect for Y198 than Y250, indicating a novel mechanism independent of an anti-oxidative function of LASSS. Neither glutathione trisulfide (GSSSG, a potent anti-oxidant) nor lipoic acid enhanced c-met binding or nitration resistance, and thus served as controls. Importantly, pre-administration of LASSS to mice prevented the disuse-induced HGF nitration observed in a tail-suspension model for muscle atrophy, while GSSSG did not. The findings encourage the idea that LASSS may react with HGF to enhance its receptor-binding affinity and nitration resistance, which are known to strongly drive myogenic stem cell dynamics and homeostasis. Application of this model could potentially lead to pioneering strategies to counteract or treat age-related muscle atrophy and impaired regeneration with fibrosis and fat infiltration (including sarcopenia and frailty).

Keywords C-Met binding affinity, Hepatocyte growth factor (HGF), Lipoic acid trisulfide (LASSS), Mouse and rat, Muscle atrophy, Peroxynitrite, Resident myogenic stem satellite cell, Tyrosine nitration

Abbreviations

βME	β-mercaptoethanol
BrdU	5-bromo-2'-deoxyuridine
BSA	Bovine serum albumin
DAB	3,3'-diaminobenzidine

[1]Department of Animal and Marine Bioresource Sciences, Graduate School of Agriculture, Kyushu University, West Zone 5, Motooka 744, Nishi-ku, Fukuoka 819-0395, Japan. [2]Department of Physiology, Faculty of Veterinary Medicine, Kafrelsheikh University, El-Geish Street, Kafrelsheikh 33516, Egypt. [3]Department of Bioscience and Biotechnology, Graduate School of Agriculture, Kyushu University, West Zone 5, Motooka 744, Nishi-ku, Fukuoka 819-0395, Japan. [4]Department of Food and Life Science, School of Life and Environmental Science, Azabu University, Sagamihara 252-5201, Japan. [5]Department of Animal Science and Biotechnology, School of Veterinary Medicine, Azabu University, Sagamihara 252-5201, Japan. [6]Department of Biological Sciences, Faculty of Science, University of Manitoba, Winnipeg, MB R3T 2N2, Canada. [7]Kahona Zushi and Miyumi Seki have contributed equally to this work. ✉email: rtatsumi@agr.kyushu-u.ac.jp

DMEM	Dulbecco's modified Eagle's medium
ECL	Enhanced chemiluminescence
GSSSG	Glutathione trisulfide
HGF	Hepatocyte growth factor
HRP	Horseradish peroxidase
HS	Horse serum
mAb	Monoclonal antibody
LASSS	Lipoic acid trisulfide
SDS	Sodium dodecyl sulfate
TTBS	Polyethylene sorbitan monolaurate (Tween20)-Tris-buffered saline
Y	Tyrosine residue

Several studies have demonstrated that hepatocyte growth factor (HGF) displays critical functions in development, regeneration and repair of a variety of tissues and organs[1–17]. Our previous studies revealed the essential role of HGF in mechano-biology of postnatal muscle growth and regeneration centered on resident myogenic stem satellite cells, which are positioned between the basal lamina and the sarcolemma of postnatal myofibers and normally found in a mitotically and metabolically quiescent or near-dormant state (protracted G_1 phase, also referred to G_0) in adult muscle. Briefly, when muscle is injured, overused, or mechanically stretched, satellite cells are activated to enter the cell cycle through a cascade of events including nitric oxide (NO) radical-dependent release of the active form of HGF (a hetero-dimer of α- and β-chains) from its extracellular tethering and the subsequent presentation of HGF to the cell-membrane signaling receptor c-met, followed by the sequence of steps including proliferation to produce myoblast progeny, differentiation, and fusion with existing muscle fibers and/or to form new fibers[18–31].

Very recently, direct-immunofluorescence microscopy of rat lower hindlimb muscles revealed that with aging, extracellular matrix (ECM)-bound HGF undergoes tyrosine residue (Y) nitration, as visualized by anti-nitrated Y-HGF monoclonal antibodies (mAbs, rat clones 3A11C6 and 6B82C3 raised in-house) in experiments employing three age-groups of young (2-month-old), adult (10-month-old), and old rats (20-month-old)[32]. Notably, the age-related increases in nitration of ECM-bound HGF were predominant on fast IIa and IIx myofibers[32], corresponding with the fast fiber-preference observed in age-related muscle atrophy and impaired regeneration in humans in which fast IIb fibers are scarce[33–39].

Subsequent biochemical and cytochemical studies demonstrated that HGF nitration is maximal in a physiological pH range at Y198 and Y250, characterized by their respective locations at the c-met binding sites of the K1 and K2 domains of the HGF α-chain; their nitration resulting in a loss of c-met binding affinity of the ligand and thereby disturbs myogenic stem cell dynamics responsible for muscle homeostasis. Such nitration-dysfunction is specific to HGF among other major growth factors examined (FGF2, IGF1, and TGF-β2), highlighting the inhibitory impact of accumulation of nitrated HGF on myogenic stem cell biology during aging[32].

Protein-tyrosine nitration is a post-translational chemical modification process for the highly selective non-enzymatic introduction of a nitro group ($-NO_2$) into the side chain by peroxynitrite ($ONOO^-$), a short-lived biomolecule generated by the rapid reaction of NO with superoxide radicals in vivo[40,41]. Detrimental accumulation of specifically nitrated proteins is observed in aging[42,43] and a variety of disorders including Alzheimer's and Parkinson's diseases[44–46]. Prevention of HGF nitration-dysfunction offers novel potential to suppress the progression of age-related disorders of muscle homeostasis including muscle atrophy and impaired regeneration accompanied by up-regulation of intramuscular fibrogenesis (fibrosis) and adipogenesis (fat infiltration). Preventing HGF nitration-dysfunction could also improve the therapeutic effects of investigational HGF drugs for various diseases including liver cirrhosis, chronic renal failure, lung fibrosis, myocardial infarction, arteriosclerosis obliterans, amyotrophic lateral sclerosis (ALS, Lou Gehrig's disease), and acute spinal cord injury[47–55].

As a prototype preventive molecular tool, very recently we employed the Fab segment of the in-house-generated rat anti-HGF mAb 1H41C10 (IgG2a(κ)), raised against the synthetic peptide FTSNPEVR$_{nitro}$Y$_{198}$EV, a sequence highly conserved among mammals. This Fab segment exhibited in vitro preventive effects against peroxynitrite-induced nitration of both Y198 and Y250 in HGF, thereby preserving c-met binding and satellite cell activation[56]. In the present study, we add consideration of two trisulfides: glutathione trisulfide (GSSSG,FW: 644.70)[57,58] and lipoic acid trisulfide (LASSS,FW: 238.39; *R*-enantiomer)[59], which are both highly reactive, labile molecules having covalent bond structures with three consecutive sulfur atoms (see Figure 1a for chemical structures). Recent findings showed involvement of "supersulfides" including trisulfides, in various physiological and regulatory mechanisms characterized by their redox characteristics depending on the possible valence of the sulfur atoms[60,61]. Results clearly present the chemical potentiation of LASSS on physiological functions of HGF, as revealed by enhanced receptor-binding affinity and nitration-dysfunction resistance through interaction/reaction with LASSS under physiological conditions. Companion molecules GSSSG and lipoic acid (LASS) did not exhibit these effects, thus highlighting the unique characteristics of LASSS.

Methods

Materials

Recombinant mouse HGF (2207-HG/CF; carrier-free; disulfide-linked heterodimer of α and β chains as the major form in the product) was purchased from R&D Systems (Minneapolis, MN, USA). Peroxynitrite (P332) was purchased from Dojindo Laboratories (Kumamoto, Japan). Horseradish peroxidase (HRP)-labeled anti-nitrotyrosine (clone 39B6; sc-32757 HRP) and HRP-labeled anti-human HGF α-chain mAbs (clone H-10, sc-374422 HRP) were from Santa Cruz Biotechnology (Dallas, TX, USA). Anti-nitrotyrosine-HGF mAbs (3A11C6

anti-nitroY198-HGF and 6B82C3 anti-nitroY250-HGF) were raised in-house against a synthetic peptides FTSNPEVR$_{nitro}$Y$_{198}$EV and KFLPER$_{nitro}$Y$_{250}$PDKGFD, respectively (sites well-conserved in mammals) as described previously[32]. Glutathione trisulfide (GSSSG,$C_{20}H_{32}N_6O_{12}S_3$ dihydrate; FW: 680.73; CAS RN: 32607-79-7) and lipoic acid trisulfide (LASSS; $C_8H_{14}O_2S_3$; FW: 238.39; *R*-enantiomer; CAS RN: 1204245-29-3) were kindly provided by Kyowa Pharma Chemical Co., Ltd. (Toyama, Japan). Lipoic acid (123–06461; LA; $C_8H_{14}O_2S_2$; FW: 206.33; CAS RN: 1077-28-7) was from FUJIFILM Wako Pure Chemical (Osaka, Japan).

Dulbecco's modified Eagle's medium (DMEM; 31600-034), normal horse serum (HS; 16050-122), antibiotic-antimycotic (15240-062), and gentamicin (15710-064) were purchased from Invitrogen (Grand Island, NY, USA). Poly-L-lysine (P9155), bovine plasma fibronectin (F1141), protease type XIV (P5147), 5-bromo-2'-deoxyuridine (BrdU; B5002), HRP-labeled goat anti-mouse IgG Ab (A4416), 3,3'-diaminobenzidine (DAB; D5637), and bovine serum albumin (BSA; fraction V; A4503) were all from Sigma-Aldrich (St. Louis, MO, USA).

Recombinant mouse HGFR/c-met Fc chimera (7065-ME; carrier-free), biotinylated polyclonal anti-human HGF Ab (BAF294; antigen affinity purified), streptavidin-HRP conjugate (4800-30-06), and tetramethyl benzidine (TMB) substrate solution (DY999) were purchased from R&D systems. HRP-labeled rabbit anti-rat IgG (ab6734) was purchased from Abcam (Cambridge, MA, USA). Amersham enhanced chemiluminescence (ECL) detection kit (PRN2106) and nitrocellulose membranes (10600048) were purchased from GE Healthcare (Little Chalfont, UK). Monoclonal anti-BrdU (clone G3G4) and anti-desmin Abs (clone D3) were purchased from Developmental Studies Hybridoma Bank (Iowa City, IA, USA). Amicon Ultra-0.5 ultrafiltration device (UFC5010; equipped with 10-kDa MWCO regenerated cellulose membrane) was purchased from Merk (Darmstadt, Germany).

Animal care and use

All experiments involving animals were conducted in strict accordance with the recommendations in the Guidelines for Proper Conduct of Animal Experiments published by the Science Council of Japan and ethics approvals from the Kyushu University Institutional Review Board (approval No. A20-014, A22-082, A24-254, A28-092, and A30-143). Muscle tissues were collected from rats and mice after euthanasia with an overdose of isoflurane in an induction chamber. Sex as a biological variable: we utilized only male rats to maximize the satellite cell yield per gram of muscle tissue and individual animal (Figure 1d,f and supplementary Figure 1a) and male mice to examine the preventive effect of oral administration of glutathione trisulfide (GSSSG) and lipoic acid trisulfide (LASSS) (Figure 2e) on disuse-induced nitration-dysfunction of ECM-bound HGF; sex was not considered as a biological variable.

Pre-treatment of HGF with trisulfides and nitration

Recombinant mouse HGF (carrier protein-free) was pre-treated with glutathione trisulfide (GSSSG) and lipoic acid trisulfide (LASSS) at mole ratios (HGF : trisulfide) of 1:0 (with solvent alone), 1:400, 1:1000, and 1:4000 at pH 7.4, 25˚C just prior to the peroxynitrite protocol (optimized at a molar ratio 1:2000 relative to HGF, pH 7.4, 37˚C, for 30 min), which was previously demonstrated to induce maximal nitration of Y198 and Y250 located in the α-chain under physiological conditions as described previously[32]. Peroxynitrite ($ONOO^-$,0.1 M stock solution in 0.3 M NaOH-NaCl) was diluted to less than 1/100 with ice-cold water, just prior to quick exposure to HGF in PBS by vortexing at 1:2000 (see Figure 1a for the experimental design)[32]. HGF was evaluated for susceptibility to tyrosine nitration by subsequent ECL-Western blotting to detect nitrotyrosines. HGF with solvent alone (without adding peroxynitrite) was assigned as the negative control.

Ultra-filtration (to wash out un-reacted free trisulfides)

Trisulfide-pretreated HGF solutions were loaded into Amicon ultra-filtration devices (with a 10-kDa MWCO polyethersulfone (PES)-membrane) and spun at the recommended centrifugal force (typically 6000-7000 rpm) for 10–30 min at 4˚C or until the desired volume was reached. The retentate was suspended in PBS and then re-centrifuged; the process was repeated three times to efficiently remove residual trisulfides and collect HGF specimens (Figure 2a-d).

ECL-Western blotting

Tyrosine nitration was visualized by Western blotting of peroxynitrite-treated HGF according to Elgaabari et al.[32] (Figures 1b,c and 2b,c). Briefly, proteins were subjected to sodium dodecyl sulfate-10% polyacrylamide gel electrophoresis (SDS-10% PAGE) under reducing conditions in Laemmli's buffer system followed by transfer to nitrocellulose membranes[19]. Blots were incubated overnight at 4 °C with HRP-conjugated anti-nitrotyrosine mouse mAb (1:2500 dilution in CanGetSignal solution 1,NKB-101, Toyobo, Osaka, Japan), followed by ECL-detection on a FUSION SOLO.7S.EDGE imaging system (Vilber Lourmat, Marne-la-Vallée, France). Subsequently, the blots proceeded through a second round of immunodetection by agitating for 45 min at 50˚C in stripping buffer (2% SDS, 0.8% β-mercaptoethanol (βME), and 62.5 mM Tris-HCl, pH 6.8)[32,56,62] followed by re-probing with HRP-labeled anti-HGF *N*-terminal domain mAb (1:2500 dilution in CanGetSignal solution 1) to monitor HGF α-chain amount on the blots as loading controls. Further immunoblotting analysis of the nitration level of HGF was performed in the same manner using anti-nitroY198/Y250-HGF mAbs (1:2500 dilution,clones 3A11C6 and 6B82C3 raised in-house specifically to visualize nitroY198-HGF and nitroY250-HGF, respectively, see Elgaabari et al.[32] and HRP-labeled secondary antibody (immunogen-affinity purified,1:5000 dilution in CanGetSignal solution 2).

Densitograms of nitrated HGF α-chain bands were measured by ImageJ 1.34 s for linear intensity (originally developed by Dr. Wayne Rasband, National Institutes of Health, Bethesda, MD, USA) and normalized with total HGF α-chain (nitrated plus non-nitrated HGF α-chain; see Figure 2b,c), although the quantification of nitrated HGF by Western blot densitometry is semi-quantitative.

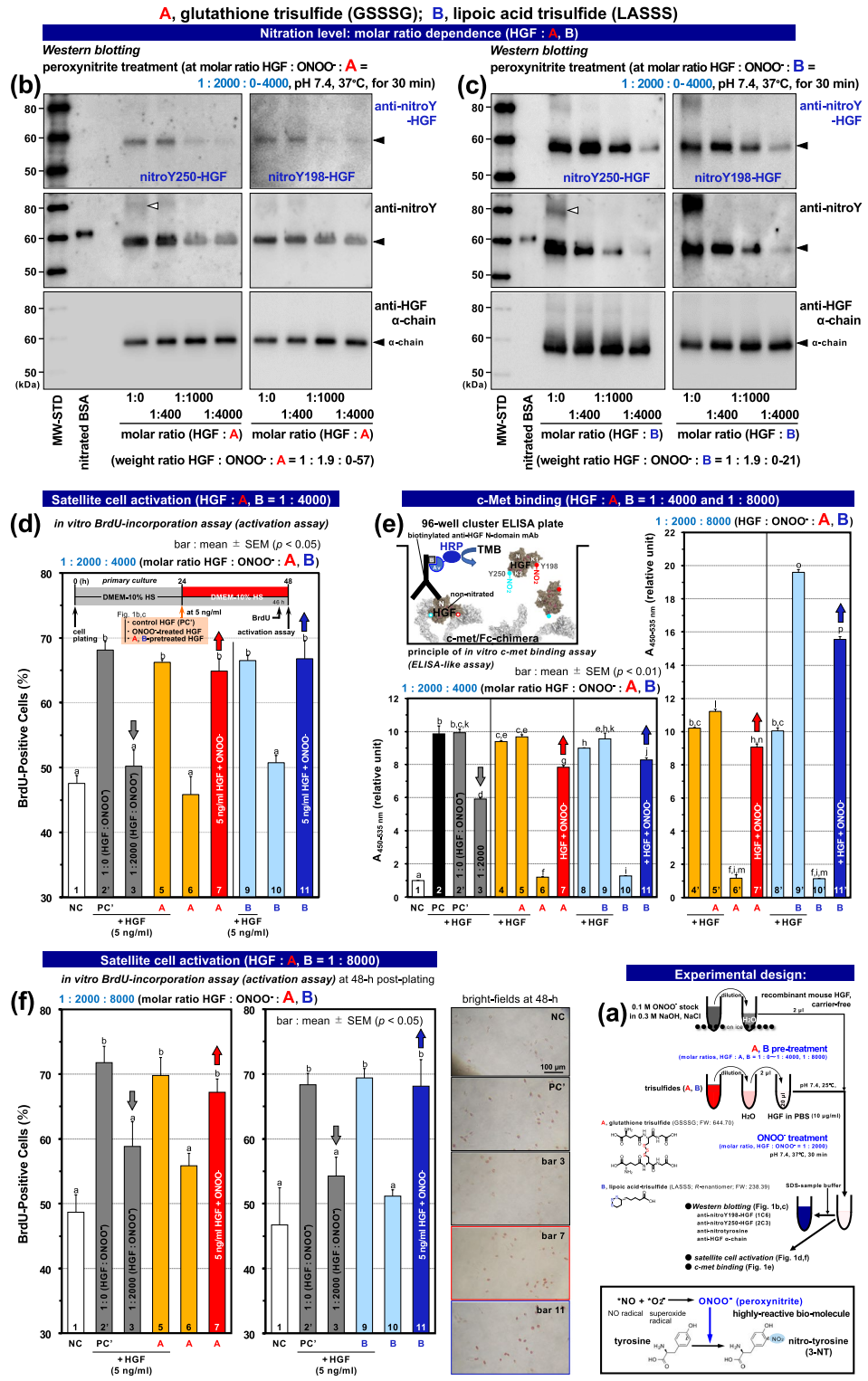

Authors ensure that gels/blots used in Figures 1b,c, 2b,c, and S2 adhere to the journal compliance with the digital image and integrity policies; original un-cropped images demonstrating full/adequate length gel and membranes (with or without visible edges) were shown in the supplementary Figures 4–7.

Satellite cell preparation and activation assay

Satellite cells were isolated from the upper hindlimb and back muscles of 9–10 month-old male Sprague-Dawley rats according to Allen et al.[63] with a slight modification[22]. Briefly, muscles were collected, trimmed of connective tissue and fat, minced with scissors, then digested with 1.25 mg/ml of protease type XIV for 1 h at 37°C. Cells were separated from muscle tissue debris by differential centrifugation and filtration (nylon cell strainers) prior to a final centrifugation step at 1500 x g for 3 min, then suspended in DMEM containing 10% normal horse serum (HS), 1% antibiotic-antimycotic mixture, and 0.5% gentamicin (DMEM-10% HS), and plated on poly-L-

◀**Fig. 1**. **Effect of pre-treatment with trisulfides on HGF-Y198/Y250 nitration (assayed without wash-out of trisulfides).** (**a**) In vitro experimental design for evaluating the effect of pre-treatment with trisulfides, glutathione trisulfide (A; GSSSG; FW: 644.7) and lipoic acid trisulfide (B, LASSS; FW: 238.39), on HGF nitration. Recombinant HGF (carrier protein-free; disulfide-linked heterodimer of 60-kDa α-chain and 30-kDa β-chain as the major form in the product) was incubated with GSSSG (A) and LASSS (B) over a range of 1:0–1:4000 (molar ratios relative to HGF) just prior to the optimized $ONOO^-$ (peroxynitrite)-protocol at a molar ratio of 1:2000 relative to HGF, pH 7.4, 37℃, for 30 min. Lower column is a sketch of nitration, the peroxynitrite-induced nitrotyrosine formation by introduction of a nitro group ($-NO_2$) into a Cε atom in aromatic ring of the side chain. (**b**) Evaluation of nitration levels of HGF pre-treated with GSSSG (A). Assayed by anti-nitroY-HGF mAbs (6B82C3 anti-nitroY250-HGF and 3A11C6 anti-nitroY198-HGF, which display high immuno-specificity to nitrated Y250-HGF and nitrated Y198-HGF, respectively, as described by Elgaabari et al.[32], in ECL-Western blotting format normalized by the total HGF α-chain detected with HRP-labeled anti-HGF α-chain mAb after stripping with SDS-βME solution (lower row), followed by re-probing with HRP-labeled anti-nitrotyrosine mAb (anti-nitroY). Nitrated bovine serum albumin (BSA) served as a control and again demonstrated high immuno-specificity of the anti-nitroY-HGF used here (left column). MW-STD, MagicMark molecular weight standards. Closed arrowheads, 60-kDa α-chain of HGF,open arrowhead, 90-kDa inactive pro-HGF (α- and β-chains). (**c**) Evaluation of nitration levels of HGF pre-treated with LASSS (B). Assayed by ECL-Western blotting as in panel b. (**d**) Cell activation response to HGF that was pre-treated with trisulfides at 1:4000 molar ratio before exposure to peroxynitrite. The experimental scheme for assays in culture is shown in upper part of the panel (*inset*). Briefly, primary cultures of rat satellite cells received 5 ng/ml HGF (control, peroxynitrite-treated, and trisulfide-pretreated HGF prior to the peroxynitrite treatment (as shown in panels b and c) in DMEM-10% HS (pH 7.2) for 24 h beginning at 24-h post-plating followed by pulse-labeling with BrdU for 2 h just prior to the 48-h time-point of the assay for cell activation (monitored by BrdU-positive cell percentage). *Open bar 1 (NC)*, negative control untreated cultures in DMEM-10% HS; *gray bar 2' (PC')*, positive control culture with recombinant HGF (plus solvent instead of peroxynitrite solution) for 24 h beginning 24-h post-plating; *gray bar 3*, cultures with nitrated HGF (peroxynitrite-treated at 1:2000 relative to HGF). *Bars 5 and 9*, cultures with HGF that received GSSSG (A) or LASSS (B) respectively, at 1:4000 molar ratio relative to HGF, without peroxynitrite treatment; *bars 6 and 10*, cultures with only GSSSG or LASSS respectively, at the same molar dose as *bars 5, 7, 9, and 11*, without peroxynitrite treatment; *bars 7 and 11*, cultures with HGF that received pre-treatment with GSSSG or LASSS respectively, at 1:4000 molar ratio, prior to the peroxynitrite treatment (at the same 1:2000 as *bar 3*). Bars represent mean ± SEM and significant differences at $p < 0.05$ are indicated by different lowercase letters on each bar. (**e**) Receptor c-met binding activity of HGF pre-treated with trisulfides before/after exposure to peroxynitrite, evaluated by sandwich ELISA-like assay on recombinant c-met-Fc chimera (see schematic diagram of the mechanism of action[32,56]. Optical $absorbance_{450–535\ nm}$ is presented by the relative value to the negative control without HGF (*NC*, *bar 1*). Left column, pre-treatment with trisulfides at 1:4000 molar ratio relative to HGF: *black bar 2 (PC) and gray bar 2'(PC')*, control HGF without any treatment or with solvent of peroxynitrite solution, respectively, served as positive controls; *gray bar 3*, nitrated HGF (peroxynitrite-treated at 1:2000 relative to HGF). *Bars 4 and 8*, control HGF that received only the solvent of GSSSG (A) or of LASSS (B) respectively, without peroxynitrite treatment; *bars 5 and 9*, HGF that received GSSSG or LASSS at 1:4000 molar ratio relative to HGF without peroxynitrite; *bars 6 and 10*, negative controls that received either GSSSG or LASSS without peroxynitrite, respectively. *Bars 7 and 11*, HGF pre-treated with GSSSG or LASSS, respectively, prior to the peroxynitrite treatment (at the same 1:2000 molar ratio as *bar 3*). Right column, pre-treatment with trisulfides at 1:8000 molar ratio relative to HGF; the experimental conditions for all *bars 4'–11'* were identical to those for *bars 4–11* (left column), with the exception of application of a two-fold higher molar dose of trisulfides. Bars represent mean ± SEM and significant differences at $p < 0.01$ are indicated by different lowercase letters on each bar. (**f**) Cell activation response to HGF pre-treated with GSSSG (A) and LASSS (B) at 1:8000 before and after exposure to peroxynitrite (1:2000). Experimental conditions were identical to panel d, with the exception of applying a two-fold higher molar dose of trisulfides. Bars represent mean ± SEM and significant differences at $p < 0.05$ are indicated by different lowercase letters on each bar. Right column, representative bright-field micrographs of 48-h cultures immuno-stained for monitoring BrdU-positive cell percentage.

lysine and fibronectin-coated plates. Cultures were maintained in a humidified atmosphere of 5% CO_2 at 37˚C for 24 h and then incubated for the next 24-h period in DMEM-10% HS additionally containing recombinant HGF that was treated with peroxynitrite with or without trisulfide pre-treatment (see Figure 1d,f). The final concentration of HGF in media was set at 5 ng/ml, which has been shown to maximally activate satellite cells in our primary culture system[19].

Cultures were pulse-labeled with 10 μM BrdU (a nucleoside analog that competes with thymidine for incorporation into DNA) in DMEM-10% HS for the final 2-h period of 48-h in culture, followed by immunocytochemistry for detection of BrdU using G3G4 anti-BrdU mAb (1:100 dilution) and HRP-conjugated anti-mouse IgG Ab (1:500 dilution). The mean percentage of BrdU-labeled cells for three cultures per treatment was used as an indicator of activation (entry into the cell cycle) and the subsequent proliferation activity of plated satellite cells, according to Tatsumi et al.[19–21]. Companion satellite-cell cultures, prepared at the same time, were immunostained at 30-h post-plating with D3 anti-desmin mAb and DAB (a chromogenic HRP-substrate that forms an insoluble brown reaction product) to determine the percentage of myogenic cells present[18,19] cultures with less than 95% DAB-positive cells (namely, less than 95% desmin-positive myogenic purity) were not used

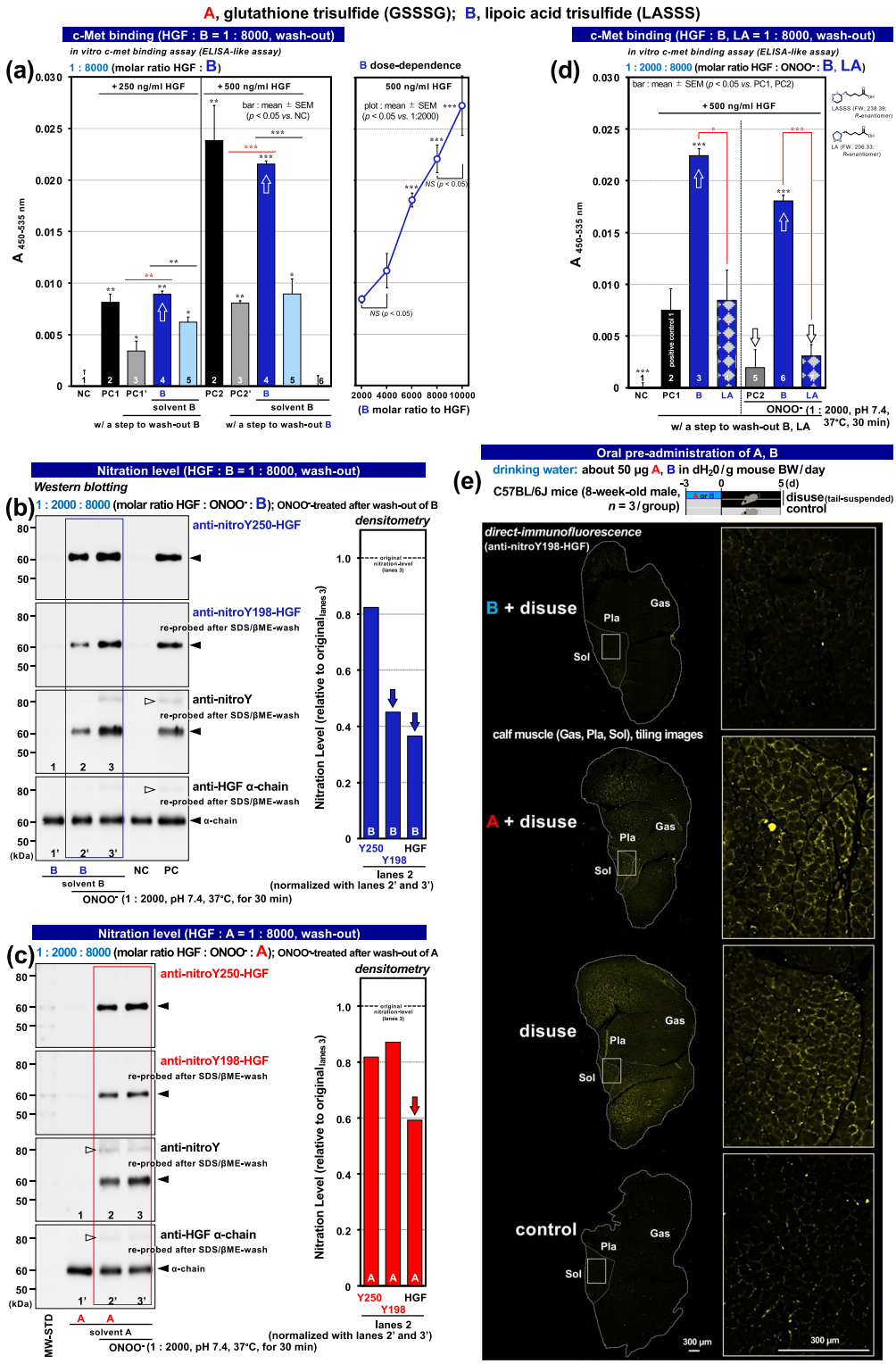

for experiments just to ensure the reliability of data specific to myogenic cells in the employed primary cell culture systems.

c-Met binding assay

According to Tatsumi et al.[21] with some minor modifications[32,56], HGF treated with trisulfide and/or peroxynitrite was evaluated for in vitro c-met binding affinity. Briefly, 96-well ELISA microplates were coated with HGFR/c-MET Fc chimera (50 ng/well), blocked with 1% BSA, 5% sucrose, and 0.05% sodium azide in PBS, and then incubated for 2 h at 37˚C with HGF samples. Plates were subsequently washed with 0.1% polyethylene sorbitan monolaurate (Tween20)-Tris-buffered saline (TTBS), immediately fixed with cold 3.7% paraformaldehyde in PBS, and re-treated with the blocking solution overnight at 4˚C. The binding of HGF to c-met was detected with biotinylated anti-HGF polyclonal Ab (1:500 dilution in the 0.1% BSA-TTBS for 3 h at 25˚C), TACS streptavidin-

◂**Fig. 2. Enhanced receptor binding-affinity and nitration resistance of HGF by lipoic acid trisulfide (at 1:8000 molar ratio, with wash-out step).** (**a**) Evaluation of receptor binding-affinity of HGF treated with/without lipoic acid trisulfide (B, LASSS; left column, at 1:8000 molar ratio to HGF). Assayed by sandwich ELISA-like format on recombinant c-met-Fc chimera as shown in Figure 1e, after wash-out of un-reacted free LASSS with centrifugal ultra-filtration device. Optical absorbance$_{450-535\ nm}$ is presented by subtracting the value of the negative control without HGF (*NC*, *bar 1*). *Black bars 2 (PC1* and *PC2)* and *gray bars 3 (PC1'* and *PC2')*, control HGF without any treatment or only with ultra-filtration step (without adding LASSS), respectively, served as positive controls in 250 ng/ml and 500 ng/ml HGF groups; differences between black and gray bars represent the protein recovery after ultra-filtration that often meets considerable protein-adsorption to the membrane. *Blue bars 4*, HGF that received LASSS (1:8000 molar ratio); *light blue bars 5*, HGF that received only the solvent of LASSS; *bar 6*, control without HGF and with solvent of LASSS. Right column, dose-dependence of receptor binding-affinity of HGF (in a range from 1:2000 to 1:10000 molar ratios of LASSS relative to 500 ng/ml HGF), assayed as in the *right-hand blue bar 4*. Bars and plots represent mean ± SEM and significant differences at $p < 0.05$, $p < 0.01$, and $p < 0.001$ are indicated by (*), (**), and (***), respectively. *NS*, not significant at $p < 0.05$. Note that the receptor c-met-binding affinity of HGF was enhanced by interaction/reaction with LASSS in a dose-dependent manner (in a molar-ratio range exceeding 1:4000) and increased more than two-fold the original at 1:8000. A comparable effect was observed in the absence of wash-out of LASSS (see Figure 1e, right column, *bars 8' and 9'*). (**b**, **c**) Evaluation of the nitration level of HGF pre-treated with LASSS (B) and GSSSG (A) at a 1:8000 molar ratio to HGF before exposure to peroxynitrite at 1:2000 (optimized molar ratio) at pH 7.4, 37℃, for 30 min. Assayed after wash-out of un-reacted trisulfides with a centrifugal ultra-filtration device as in panel a, just prior to the peroxynitrite-protocol, by ECL-Western blotting normalized by total HGF α-chain as shown in Figure 1c. *NC*, negative control HGF without any treatment; *PC*, positive control nitrated HGF (1:2000 molar ratio of peroxynitrite to HGF); *lanes 1 and 1'*, control non-nitrated HGF pre-treated with LASSS or GSSSG; *lanes 2 and 2'*, HGF that received pre-treatment with LASSS or GSSSG before exposure to peroxynitrite; *lanes 3 and 3'*, HGF that received only the solvent of LASSS or GSSSG before peroxynitrite treatment. Closed arrowheads, 60-kDa α-chain of HGF; open arrowheads, 90-kDa pro-HGF (left columns). Right columns, density scans of nitrated HGF bands were determined by ImageJ densitometry normalized with the measure of total HGF α-chain (*lanes 2' and 3'*, visualized by immuno-staining with anti-HGF α-chain mAb) and presented as relative to the original, nitrated HGF (*lanes 3*, without pre-treatment with LASSS or GSSSG and with wash-out step). MW-STD, MagicMark molecular weight standards. Note that the reaction/interaction with LASSS inhibits nitration of HGF, and the observed effect is greater for Y198 compared to Y250. (**d**) No effect of disulfide lipoic acid (LA) pre-treatment on receptor-binding affinity of HGF (assayed at same molar ratio of HGF:peroxynitrite:LA = 1:2000:8000 as in panel a, right column). Evaluated before and after nitration by sandwich ELISA-like format on recombinant c-met-Fc chimera after wash-out of residual LA and LASSS (B, served as a positive control) with centrifugal ultra-filtration device and presented by subtracting the value of the negative control without HGF (*NC*, *bar 1*), as shown in Figure 2a. Experimental conditions were same as Figure 2a. *Black bar 2 (PC1)* and *gray bar 5 (PC2)*, positive control HGF without or with exposure to peroxynitrite (at 1:2000 molar ratio to HGF), respectively. *Blue bars 3 and 6*, HGF received LASSS (at 1:8000) without or with the subsequent peroxynitrite treatment, respectively. *Blue-dotted bars 4 and 7*, HGF received LA (at the same 1:8000 molar ratio) without or with the subsequent peroxynitrite treatment, respectively. Bars represent mean ± SEM and significant differences at $p < 0.05$ and $p < 0.001$ are indicated by (*) and (***), respectively. (**e**) Evaluation of the preventive effect of glutathione trisulfide (GSSSG) and lipoic acid trisulfide (LASSS) pre-administration on muscle disuse-induced nitration of ECM-bound HGF. Assayed by direct-immunofluorescence microscopy with Fluorescein-labeled anti-nitroY198-HGF mAb (fluorescent false-yellow). Calf muscles (Sol, soleus; Pla, plantaris; Gas, gastrocnemius muscle of lower hind-limb) were collected from male mice (8–9 weeks old) in one of four experimental groups (n=3–4/group): i) control, ii) 5 days of muscle-disuse after tail suspension, and iii) and iv) 3 days pre-administration of GSSSG (A) and LASSS (B) (about 50 μg/g body weight per day in drinking water), respectively, each followed by 5 days of muscle disuse without the GSSSG and LASSS supplementation. Cryo-sections of calf muscle (mid-belly portion, 15-μm thickness) were blocked with sterile donkey serum/BSA/gelatin solution prior to incubation with HiLyte Fluor 647-labeled anti-nitrated Y198-HGF. Representative images of each group are shown. Right column, high magnification views of boxed areas in Sol (left column, tiling images), a muscle abundant in slow and fast IIa fibers.

HRP conjugate (1:1600 dilution for 20 min), and TMB substrate solution. After stopping the coloration reaction, optical density measurements were taken at wavelengths of 450 and 545 nm (Figures 1e and 2a,d).

Trisulfide oral-administration to mice (in vivo experiments)

Effect of glutathione trisulfide (GSSSG) and lipoic acid trisulfide (LASSS) pre-administration on muscle disuse-induced nitration of ECM-bound HGF[64] was evaluated by direct-immunofluorescence microscopy with HiLyte Fluor 647-labeled anti-nitroY198-HGF mAb (clone 3A11C6,fluorescent false-yellow). Calf muscles (soleus, plantaris, and gastrocnemius muscles of lower hind-limb) were collected from male C57BL/6J mice (8-weeks old) of four experimental groups (n=3/group): control, 5 days of muscle-disuse induced by tail suspension, and 3 days pre-administration of GSSSG or LASSS (about 50 μg/g body weight per day in drinking water) followed by 5-days muscle disuse without the GSSSG and LASSS supplementation. Mice received water and diet (CRF-1; Oriental Yeast, Tokyo, Japan) ad libitum during the experimental period; there was no significant difference in either body-weight gain or total food intake (per g body weight) among four experimental groups (data not

shown). Cryo-sections of calf muscle (mid-belly portion, 15-μm thickness) were blocked with sterile donkey serum/BSA/gelatin solution prior to incubation with HiLyte Fluor 647-labeled anti-nitroY198-HGF mAb (clone 3A11C6; fluorescent false-yellow). Sections were mounted in VECTASHIELD Antifade Mounting Medium and observed under a KEYENCE BZ-X700 fluorescence microscope equipped with a digital camera and a Tile-Scan program (Figure 2e).

Statistical analyses

Post-hoc Tukey's tests were employed for statistical analysis of experimental results. Data are represented as mean ± standard error of the mean (SEM). The level of significance was set to $p < 0.05$ throughout this study and statistically significant differences between two groups are indicated on graphs by different lowercase letters on each bar or by (*) at $p < 0.05$, (**) at $p < 0.01$, and (***) at $p < 0.001$, respectively. The results are representative examples of more than two or three independent experiments.

Results

Anti-nitrative effect of trisulfides as an introductory part of the study

Given the potent anti-oxidative functions of GSSSG and LASSS, the first set of experiments was designed to examine if these trisulfides have potential to prevent peroxynitrite-induced nitration-dysfunction of HGF by ECL-Western blotting (see Figure 1a for the in vitro experimental design). Recombinant mouse HGF (carrier protein-free) was incubated with GSSSG (A) and LASSS (B) at molar ratios ranging from 1:0 to 1:4000 relative to HGF (corresponding to weight ratios of 1:0 to 1:57 and 1:0 to 1:21 with A and B, respectively) just prior to the optimized peroxynitrite-protocol at a molar ratio 1:2000 relative to HGF, pH 7.4 (Figure 1b,c). Results clearly showed that the tyrosine-nitration level was reduced in proportion to the molar ratios of GSSSG and LASSS relative to HGF, as revealed by the decrease in anti-nitroY mAb-positive HGF (60-kDa α-chain and 90-kDa proform) normalized to total HGF α-chain as a loading control, that was monitored by stripping with SDS-βME solution and re-probing the blot with anti-HGF α-chain N-terminal domain mAb (Figure 1b,c, second and third rows). Importantly, decreased Y198- and Y250-nitration was visualized by re-probing the blots with 3A11C6 anti-nitroY198-HGF and 6B82C3 anti-nitroY250-HGF-specific mAbs, respectively (Figure 1b,c, first rows). An additional set of blots of nitrated bovine serum albumin (BSA) showed an immuno-positive response to anti-nitroY mAb while not to anti-nitroY250-HGF mAb, and hence served as a control and demonstrated high immuno-specificity of the anti-nitroY-HGF used here. These results demonstrate that GSSSG/LASSS-pretreated HGF displays resistance to Y198, 250-nitration in vitro, encouraging the notion that the two molecules have therapeutic availability.

This issue was further examined by evaluating the impact of HGF treated by GSSSG or LASSS on activation of myogenic stem satellite cells in culture (Figure 1d). Primary cultures of satellite cells were prepared from the upper hindlimb and back muscles of 9–10 month-old male rats and cultured for 24 h beginning at 24-h post-plating in DMEM-10% HS containing 5 ng/ml HGF that was pre-treated with GSSSG and LASSS separately at 1:4000 molar ratio just prior to peroxynitrite treatment (1:2000 to HGF; see panel d inset for the culture design). The activation index in each condition was evaluated by determining the percentage of bromodeoxyuridine (BrdU)-positive cells, indicative of the cell-activation response to HGF samples. Results clearly showed that the activation index was rescued up to a level comparable to a positive control culture (*bar 2'*) exposed to untreated HGF at the 5 ng/ml dose that maximizes satellite cell activation in our culture platform (*bars 7 and 11*)[19]. Nitrated HGF (*bar 3*, peroxynitrite-treated at 1:2000) lost its activation activity as demonstrated by a drop in the activation index down to the baseline level observed in the negative-control culture (*bar 1*)[32] and in GSSSG/LASSS-cultures (*bars 6 and 10*, missing HGF). GSSSG and LASSS alone did not affect the activation index of "regular" HGF (*bars 5 and 9*, peroxynitrite-untreated). These experiments provide a robust demonstration that GSSSG and LASSS treatment of HGF prevents peroxynitrite-induced Y198/Y250-nitration/dysfunction of HGF, and thus guarantee satellite cell activation activity.

The finding was further supported by c-met-binding experiments, in which HGF was pre-treated with GSSSG and LASSS at the same molar ratio 1:4000 at which the satellite-cell activation index was rescued to a level comparable to that of non-nitrated "regular" HGF, as shown in Figure 1d, followed by exposure to peroxynitrite (1:2000) and evaluated for c-met-binding by a sandwich ELISA-like assay on recombinant c-met-Fc chimera (Figure 1e, left column; see schematic diagram of mechanism). The assay was designed to demonstrate the biochemical activity of c-met binding sites including Y198 and Y250 (in K1 and K2 domains of HGF, respectively) by significant changes in optical absorbance (expressed as relative unit) within a range from a baseline level (a negative control without HGF; *bar 1*) to a positive control level (non-nitrated HGF; *bars 2 and 2'*). Binding affinity of the GSSSG/LASSS-pretreated HGF (*bars 7 and 11*) to c-met was significantly higher than that of nitrated HGF (*bar 3*, peroxynitrite-treated at 1:2000) and reached approximately 80% of the full activity of the positive controls exposed to untreated HGF (*bars 2 and 2'*). Treatment groups with GSSSG (*bars 5 and 6*), LASSS (*bars 9 and 10*), or their solvents alone (*bars 4 and 8*) did not affect HGF binding to c-met. In conclusion, we demonstrated in the first half of Figure 1 that pre-treatment with GSSSG or LASSS effectively prevents nitration of HGF-Y198, Y250, thereby preserving the ability of HGF to activate myogenic stem satellite cells in vitro through the c-met signaling pathway (panels b-d and panel e left column).

Unique functions of LASSS

The finding of the anti-nitrative function of GSSSG and LASSS observed at the 1:4000 molar ratio constitutes an introductory part of the present study and importantly led to conducting pilot experiments to investigate the impacts of GSSSG and LASSS at higher molar ratio (1:8000) on c-met binding and satellite cell activation (Figure 1 panel e, right column, and panel f). Under the same experimental format as Figure 1e left column, except using a molar ratio of GSSSG and LASSS to HGF (1:8000), LASSS-treated HGF (Figure 1e right column, *bar*

9') displayed about 2-fold higher c-met binding than the control HGF level (*bar 8'*, in which HGF just received the solvent) equivalent to the positive controls (*bars 2 and 2'* in the left column). Even when LASSS-pretreated HGF was exposed to peroxynitrite (*bar 11'*; at the same 1:2000 as before), the c-met binding index was still higher than the control HGF (*bar 8'*) and the "original" LASSS/peroxynitrite-pretreated HGF (1:4000; *bar 11* in the left column). Notably, the control LASSS treatment (*bar 10'*, missing HGF) exhibited a low activation index equivalent to the baseline level (*bar 1* in the left column), indicating that LASSS does not, itself, stimulate c-met signaling directly. In contrast to the remarkable LASSS effect observed, GSSSG treatment did not modulate HGF-c-met interaction either before or after HGF exposure to peroxynitrite (though a subtle increase was statistically significant; see differences between *bars 5 and 5'* and between *7 and 7'*), as visualized by comparable indices between 1:4000 (*bars 4–7*) and 1:8000 experimental groups (*bars 4'–7'*). In primary culture of satellite cells, the LASSS-treated HGF (Figure 1f, *bars 9 and 11*, at 5 ng/ml without or with exposure to peroxynitrite, respectively) normally activates satellite cells to a level equivalent to the positive control (*bar 2'*) as revealed by BrdU-incorporation assay. These results all encourage a conclusion that LASSS treatment (at 1:8000 ratio to HGF) may enhance the c-met binding-affinity of HGF without disturbing HGF-c-Met signaling and that this enhancement occurs through a mechanism that is unrelated to prevention of HGF nitration. This conclusion further highlights a specific performance of LASSS to extend or amplify the availability of LASSS-HGF.

This insight was further supported by two sets of supplemental experiments. i) LASSS-treated HGF, at as low as 1 ng/ml that is below 2.5–10 ng/ml of the optimal final-concentration range in culture media (supplementary Figure 1a, *left light-blue bar*), activates satellite cells to the maximum level presented by the positive control (*black bar PC*, 5 ng/ml HGF). The counter GSSSG treatment did not increase activation activity of 1 ng/ml HGF (*left orange-bar*), consistent with the earlier observation that GSSSG did not effectively modulate the HGF-c-met interaction (Figure 1e right column, *orange bars 4' and 5'*), and hence served as a control trisulfide. The LASSS-untreated "original" HGF (supplementary Figure 1a, *gray bar PC*'; at the same 1 ng/ml) displayed lower activation activity than the maximum level of the LASSS-treated HGF, aligning with the established HGF-dose-dependent manner of satellite cell activation with maximum at 2.5–10 ng/ml on the same in vitro assay platform (see Figure inset, reproduced from Tatsumi et al.[19] and Yamada et al.[65]. In addition, the characterized LASSS treatment did not stimulate autolysis of HGF as monitored by SDS-PAGE for degradation of 60-kDa α-chain and 90-kDa proform of recombinant HGF incubated with LASSS (at 1:8000) at 25℃ for 2 h (see supplementary Figure 1b), providing another important basis for the availability of LASSS-HGF. ii) Primary culture of satellite cells with 5 ng/ml HGF, which received only the LASSS pre-treatment (at 1:8000, without peroxynitrite treatment), exhibited a cell-proliferation activity (evaluated by mRNA expression levels of MyoD and its counter-regulatory factor myogenin at 48-h and 72-h time-points) comparable to that of the positive control culture treated with 5 ng/ml control HGF without LASSS (just with the solvent; data not shown).

The subsequent experiments were designed to characterize a mechanism for LASSS-enhanced c-met binding-affinity of HGF (Figure 2a). Recombinant HGF was treated only with LASSS (at the same 1:8000 molar ratio to HGF as described earlier, without exposure to peroxynitrire) and then applied to centrifugal ultra-filtration (10-kDa MWCO) to thoroughly wash out un-reacted, free LASSS (FW: 238.39) prior to the c-met binding assay. This additional step was imperative for conducting direct evaluation of the hypothesis that LASSS interacts/reacts with HGF to augment its c-met binding affinity. In the context of a restricted assay-format, in which implication of free LASSS can be excluded, the outcomes may provide critical insights towards understanding of an underlying LASSS-driven mechanism.

C-met binding was examined at two HGF-doses (250 ng/ml and 500 ng/ml in PBS) by sandwich ELISA-like assay on recombinant c-met-Fc chimera as in Figure 1e, and significant changes in optical absorbance subtracted by a baseline level (negative control without HGF, *bar 1*) were depicted in Figure 2a (left column). Results clearly showed that the c-met-binding of LASSS-treated HGF (*blue bars 4*) was more than double that of the control level of HGF (*gray bars 3*, with the wash-out step); this result is similar to the findings shown in Figure 1e, right column (*bars 8' and 9'*, missing the wash-out step). Another control-HGF group (*light-blue bars 5*, receiving a solvent followed by the wash-out step) also displayed a low activation index comparable to the level of the control HGF (*gray bars 3*), indicating again that the solvent of LASSS is not involved in the mechanism that elevates c-met binding, as shown in Figure 1e, right column. The control HGF without the wash-out step (*black bars 2*) presented higher indices than the levels of regular control HGF at both HGF doses (also see *gray bars 3* with wash-out step); this discrepancy is reasonable considering the yield of HGF after a wash-out step that often causes trapping/stacking of proteins on ultra-filtration membranes. These results help understand the methodological practicability of ultra-filtration to wash out un-reacted LASSS from the LASSS-treated HGF specimens.

Importantly, results also demonstrated that the enhancement effect of LASSS on the c-met binding-affinity of HGF is consistently maintained, even after the removal of un-reacted free LASSS (and any degradation products of LASSS), by an interaction between HGF and LASSS or potentially by specific chemical modification of HGF at a high molar ratio of 1:8000 to HGF (over 1:4000). The LASSS-stimulated mechanism is un-related to prevention of HGF nitration because all of the findings (shown in Figure 1e right panel, *bars 8'–10'* and Figure 2a) were obtained under nitration-free conditions (omitting peroxynitrite treatment). GSSSG (FW: 644.70), which has also exhibited a potent preventive effect on HGF nitration (Figure 1b), did not show an enhancement of c-met binding with HGF, as described earlier (Figure 1e *bars 4'–7'*), directly encouraging the notion that there is a nitration-independent mechanism centered on the unique characteristics of LASSS on HGF.

The impact of this insight was further extended by the finding that the LASSS-treated HGF (after the wash-out of un-reacted LASSS) exhibited nitration resistance to the optimal peroxynitrite-treatment (at the same 1:2000 ratio as before) as shown in Figure 2b. It is necessary to acknowledge that this mechanism is totally distinct from the previous observation of the preventive effect of LASSS on HGF nitration (1:4000 ratio, without the wash-out of un-reacted LASSS; see again Figure 1c). To summarize briefly, Figure 2b clearly demonstrated

that the level of HGF nitration was drastically decreased by LASSS-pretreatment as shown by Western blotting visualized by anti-nitroY mAb-positive bands normalized by total HGF α-chain (third row *lanes 2 and 3* and fourth row *lanes 2' and 3'*). This finding accounts for the important observation that the c-met binding affinity of LASSS/peroxynitrite-treated HGF (at the 1:8000:2000 molar ratio to HGF, with the wash-out of un-reacted free LASSS) was significantly higher than the original level of un-treated positive control HGF (Figure 2d, *bars 2 and 6*). Notably, the LASSS-pretreatment displayed greater preventive effect on nitration of Y198 compared to Y250, as revealed by re-probing with anti-nitroY198 and Y250-HGF mAbs (Figure 2b, first and second rows, *lanes 2 and 3*; also see the right column for densitometric analyses of nitrated HGF α-chain bands presented in arbitrary units relative to the original nitrated-HGF without LASSS pre-treatment).

The same set of experiments was conducted for GSSSG-pretreated HGF as a control and results indicated a nearly negligible preventive-effect on HGF nitration (Figure 2c), consistent with the earlier observation that GSSSG treatment barely enhanced HGF-c-met interaction before and after exposure to peroxynitrite (see again Figure 1e, *bars 4–7 and bars 4'–7'*). The substantial impact of LASSS pre-treatment was more pronouncedly demonstrated by an alternative experiment using the disulfide lipoic acid (LA, containing two sulfur atoms connected by a disulfide bond); LA pre-treatment (at 1:8000 ratio, with the wash-out step) did not affect the c-met binding-affinity of HGF before or after exposure to peroxynitrite at the same 1:2000 ratio as the LASSS pre-treatment (Figure 1d, *lanes 4 and 7*).

In vivo demonstration

Conceptual extension of emerging in vitro findings was performed by testing the potential effect of oral LASSS administration on prevention of muscle disuse-induced nitration-dysfunction of ECM-bound HGF (at Y198 and Y250 in K1 and K2 domains, respectively)[64]. Disuse-induced nitration was examined by using the 5-day tail-suspension model for hind-limb muscle inactivity. In this experimental platform, the anti-gravity calf-muscle group (gastrocnemius (Gas), plantaris (Pla), and soleus (Sol) muscles) and shank muscles (tibialis anterior (TA) and extensor digitorum longus (EDL)) were collected from four experimental groups of 8-week-old C57BL/6J male mice: i) control (without any treatment), ii) 5-days suspension-disuse, iii) 3-days LASSS pre-administration (about 50 μg in drinking water/g body weight/day) followed by 5-days suspension-disuse treatment without LASSS supplementation, and iv) 3-days GSSSG pre-administration followed by suspension-disuse treatment ($n = 3$ mice per group). Muscles were evaluated for nitration levels of ECM-bound HGF by direct-immunofluorescence microscopy with HiLyte Fluor 647-labeled anti-nitrated Y198-HGF mAb (clone 3A11C6, fluorescent false-yellow) in cross-sections of specimens (Figure 2e). Nitrated HGF was detected at the periphery of myofibers with a remarkable increase observed in the disuse group for plantaris, soleus, and gastrocnemius (anterior-lateral aspect of medial and lateral heads and the mid-body portion; see third row). Importantly, as shown in the first row, LASSS supplementation effectively prevented an increase in the nitration level of ECM-HGF, whereas GSSSG did not demonstrate efficacy, inconsistent with its potent potential shown in in vitro experiments described earlier (see Figure 1b).

The physiological signature of muscle disuse in the mice was represented by a trend toward decreased soleus muscle weight ($p = 0.084$ vs. the control group), but no change in shank muscle weight. These results are consistent with the major features of hind-limb suspension-related phenotypes of skeletal muscles as an index of anti-gravity muscle atrophy[66], thus assuring that the experimental design including the mouse age and muscle-disuse period (in vivo assay time-point) were appropriate to the conclusion that 3-days LASSS oral-administration prevents tyrosine-residue nitration of extracellular HGF (Y198) during 5-days muscle disuse. Considering again that the myogenic stem cell activator HGF is found in an ECM-bound state[19–22,26] and undergoes nitration of tyrosine residues (Y198 and Y250) with aging[32,32,62] and muscle disuse (Kuwakdo et al., 2025), the present in vivo experiments provide a robust platform showing the potential for LASSS that could efficiently reduce or delay the nitration-dysfunction of ECM-bound HGF under peroxynitrite-generating conditions.

Discussion

We demonstrated in the first part of the present work that both glutathione trisulfide (GSSSG) and lipoic acid trisulfide (LASSS) have potent redox characteristics that prevent nitration of Y198 and Y250 of the HGF α-chain, thereby preserving the ability of HGF to bind to the receptor c-met and hence activate myogenic stem satellite cells in vitro (Figure 1b-d, and Figure 1e left column). Notably, LASSS displayed additional functions to promote receptor binding-affinity and nitration resistance of HGF in a dose-dependent manner, that is high-dose LASSS in excess of a 1:4000 molar ratio to HGF, as revealed by biochemical assays after wash-out of un-reacted free LASSS (Figure 2a-d). Neither the disulfide lipoic acid (LA) nor GSSSG worked in this manner, and thus served as reliable controls in the high-dose experiments (Figure 1e *bars 4'–7'* and Figure 2c,d). These new findings encourage a novel working hypothesis for further research, that a chemical-modification mechanism enables transformation of HGF through interaction or reaction with LASSS under physiological conditions, resulting in the retention of HGF's biological activity after exposure to peroxynitrite, at least until an enhanced form of HGF undergoes metabolic turnover in vivo. This finding provides a possible explanation for the in vivo demonstration that LASSS pre-administration prevents nitration of extracellular HGF during 5-days muscle disuse (without LASSS supplementation during disuse) while the control GSSSG pre-administration does not. Importantly, an additional experiment showed that LASSS-treated BSA (after the removal of un-reacted LASSS) exhibited nitration resistance to the optimal peroxynitrite-treatment (1:2000 ratio), as shown in supplementary Figure 2, suggesting a model that LASSS-induced chemical modification mechanism exerts a nitration-inhibitory effect on a wide range of proteins susceptible to tyrosine nitration.

Considering a three-dimensional structural model for a complex of the human HGF-NK2 segment sandwiched by c-met receptor molecules (see supplementary Figure 3, re-produced from PDB ID 7MO7[67], it is hypothesized that the disulfide bonds, notably Cys149-Cys189 and Cys177-Cys201 localized internally just

behind Y198, are the targets of LASSS. According to the working model, these cysteine residues may undergo chemical modification/remodeling including trisulfide bond formation and/or related reactions, resulting in a regional (minor, but effective) structural alteration that enhances c-met binding and the nitration resistance of Y198-HGF. LASSS may be more easily accessible to the aforementioned internal disulfide bonds than GSSSG because LASSS (FW: 238.39) is about one-third the size of GSSSG (FW: 644.70). Additionally, the cyclic trisulfide structure of LASSS, as opposed to the linear trisulfides such as GSSSG and cysteine trisulfide (Cys-SSS-Cys), could guarantee the unique reactivity of LASSS (see again Figure 1a for chemical structures). These considerations have potential to account for the important observation that the LASSS-pretreatment displayed greater preventive effect on nitration of Y198 compared to Y250 (Figure 2b). Y250 is located much farther from the disulfide bonds (Cys128-Cys206 in the hinge region between K1 and K2 domains, and Cys211-Cys288, Cys232-Cys271, and Cys260-Cys283 in the K2 domain) than the distances between Y198 and disulfide bonds, Cys149-Cys189 and Cys177-Cys201. For these reasons, a Y250-containing site is likely to be less sensitive to the impacts of hypothetical chemical modification/remodeling of the disulfide bonds mentioned. Nonetheless, the present study does not directly identify the chemical modification, the modified residues/bonds, or the structural mechanism, all of which await further study.

The present work encourages additional in vivo research on the potential application of LASSS in extracellular HGF nitration-dysfunction during aging. Further exploration could lead to strategies for its use in age-related atrophy and impaired regeneration, although at this stage we have not provided direct evidence that LASSS oral-supplementation can mitigate sarcopenia or has therapeutic value, awaiting the results of aging experiments. The mechanisms have potential for use in developing new pharmaceutical strategies to maintain HGF functions in many pathological conditions. In particular, combating age-related muscle atrophy such as in sarcopenia and frailty, could extend the expectation of sustained muscle health into old age by improving human, livestock, and companion-animal welfare and sustaining food security through meat-animal production. Additionally, HGF displays pleiotropic functions in a variety of tissues and organs and therapeutic applications of investigational HGF drugs (application of new drugs developed on the basis of these HGF-mediated effects, for clinical therapy) have been tested in various diseases as described before. Chemical promotion of HGF functions (enhanced receptor binding-affinity and nitration resistance) opens a new perspective from which the therapeutic effectiveness of HGF drugs and their effective tissue-specific delivery could be improved. This LASSS-HGF strategy could be adaptable to aging[32,41,42,68–70] and several disorders and diseases that show the generation and accumulation of nitrated HGF and particular nitrated proteins at specific sites, including cardiovascular damage[71,72], chronic obstructive pulmonary disease (COPD)[73], colon and lung cancer[74–76], Alzheimer's and Parkinson's diseases[44–46,77,78].

Summary

Previously, we demonstrated age-related nitration-dysfunction of ECM-bound HGF (myogenic stem cell activator), preferentially in fast myofibers. Here we show that under our experimental conditions in vitro, HGF adopts an enhanced form with dynamically increased receptor-binding affinity and nitration-dysfunction resistance through interaction with lipoic acid trisulfide (LASSS). Notably, disulfide bonds at Cys149-Cys189 and Cys177-Cys201 residues could be potential targets of LASSS modification/remodeling. This knowledge now opens novel ways to improve interventions that could combat age-related muscle atrophy and impaired regeneration with fibrosis and fat infiltration (including sarcopenia and frailty).

Data availability

Data generated and analyzed in this study are included in the paper and the Supporting Information (supplementary Figures 1-7 and legends), and are also available to interested person from the corresponding author upon reasonable request.

Received: 12 February 2026; Accepted: 30 June 2026
Published online: 24 July 2026

References

1. Honda, S. et al. Localization and functional coupling of HGF and c-Met/HGF receptor in rat brain: Implication as neurotrophic factor. *Brain Res. Mol. Brain Res.* **32**(2), 197–210. https://doi.org/10.1016/0169-328x(95)00075-4 (1995).
2. Kawaida, K., Matsumoto, K., Shimazu, H. & Nakamura, T. Hepatocyte growth factor prevents acute renal failure and accelerates renal regeneration in mice. *Proc. Natl. Acad. Sci. U. S. A.* **91**(10), 4357–4361. https://doi.org/10.1073/pnas.91.10.4357 (1994).
3. Nakamura, T. (1994). Hepatocyte growth factor as mitogen, motogen and morphogen, and its roles in organ regeneration. *Princess Takamatsu Symp*, 24, 195-213. University of Tokyo Press.
4. Ohmichi, H. & Matsumoto, K. Nakamura, T. In vivo mitogenic action of HGF on lung epithelial cells: Pulmotrophic role in lung regeneration. *Am J Physiol Lung Cell Mol Physiol* **270**, L1031–L1039. https://doi.org/10.1152/ajplung.1996.270.6.L1031 (1996).
5. Anderson, J. E. et al. The role of semaphorin3A in myogenic regeneration and the formation of functional neuromuscular junctions on new fibres. *Biol. Rev. Camb. Philos. Soc.* **92**(3), 1389–1405. https://doi.org/10.1111/brv.12286 (2017).
6. Desole, C. et al. HGF and MET: From brain development to neurological disorders. *Front. Cell Dev. Biol.* **9**, 683609. https://doi.org/10.3389/fcell.2021.683609 (2021).
7. Lee, N., Kim, S. & Lee, J. Impairment of peripheral nerve regeneration by insufficient activation of the HGF/c-Met/c-Jun pathway in aged mice. *Heliyon* **8**(11), e11411. https://doi.org/10.1016/j.heliyon.2022.e11411 (2022).
8. Masuda, T. et al. Combined administration of BMP-2 and HGF facilitate bone regeneration through angiogenic mechanisms. *J. Hard Tissue Biol.* **24**(1), 7–16. https://doi.org/10.2485/jhtb.24.7 (2015).
9. Matsumoto, K., Funakoshi, H., Takahashi, H. & Sakai, K. HGF-Met pathway in regeneration and drug discovery. *Biomedicine* **2**(4), 275–300. https://doi.org/10.3390/biomedicines2040275 (2014).
10. Panganiban, R. A. & Day, R. M. Hepatocyte growth factor in lung repair and pulmonary fibrosis. *Acta Pharmacol. Sin.* **32**(1), 12–20. https://doi.org/10.1038/aps.2010.90 (2011).

11. Park, J. S., Kim, D. & Hong, H. S. Priming with a combination of FGF2 and HGF restores the impaired osteogenic differentiation of adipose-derived stem cells. *Cells* **11**(13), 2042. https://doi.org/10.3390/cells11132042 (2022).
12. Tatsumi, R. et al. Possible implication of satellite cells in regenerative motoneuritogenesis: HGF upregulates neural chemorepellent Sema3A during myogenic differentiation. *Am. J. Physiol. Cell Physiol.* **297**(2), C238–C252. https://doi.org/10.1152/ajpcell.00161.2009 (2009).
13. Tatsumi, R. et al. Slow-myofiber commitment by semaphorin 3A secreted from myogenic stem cells. *Stem Cells* **35**(7), 1815–1834. https://doi.org/10.1002/stem.2639 (2017).
14. Wang, Z. et al. Antifibrotic effects of hepatocyte growth factor on endothelial-to-mesenchymal transition via transforming growth factor-beta1 (TGF-β1)/Smad and Akt/mTOR/P70S6K signaling pathways. *Ann Transplant* **23**, 1–10. https://doi.org/10.12659/aot.906700 (2018).
15. Yun, Y.-R. et al. Administration of growth factors for bone regeneration. *Regen Med* **7**(3), 369–385. https://doi.org/10.2217/rme.12.1 (2012).
16. Zhang, X.-J. et al. Angiocrine hepatocyte growth factor signaling controls physiological organ and body size and dynamic hepatocyte proliferation to prevent liver damage during regeneration. *Am. J. Pathol.* **190**(2), 358–371. https://doi.org/10.1016/j.ajpath.2019.10.009 (2020).
17. Zhao, Y., Ye, W., Wang, Y.-D. & Chen, W.-D. HGF/c-met: A key promoter in liver regeneration. *Front Pharmacol* **13**, 808855 (2022).
18. Allen, R. E., Sheehan, S. M., Taylor, R. G., Kendall, T. L. & Rice, G. M. Hepatocyte growth factor activates quiescent skeletal muscle satellite cells in vitro. *J Cell Physiol* **165**(2), 307–312. https://doi.org/10.1002/jcp.1041650211 (1995).
19. Tatsumi, R., Anderson, J. E., Nevoret, C. J., Halevy, O. & Allen, R. E. HGF/SF is present in normal adult skeletal muscle and is capable of activating satellite cells. *Dev. Biol.* **194**(1), 114–128. https://doi.org/10.1006/dbio.1997.8803 (1998).
20. Tatsumi, R., Sheehan, S. M., Iwasaki, H., Hattori, A. & Allen, R. E. Mechanical stretch induces activation of skeletal muscle satellite cells in vitro. *Exp. Cell Res.* **267**(1), 107–114. https://doi.org/10.1006/excr.2001.5252 (2001).
21. Tatsumi, R., Hattori, A., Ikeuchi, Y., Anderson, J. E. & Allen, R. E. Release of hepatocyte growth factor from mechanically stretched skeletal muscle satellite cells and role of pH and nitric oxide. *Mol. Biol. Cell* **13**(8), 2909–2918. https://doi.org/10.1091/mbc.e02-01-0062 (2002).
22. Tatsumi, R. et al. Low-pH preparation of skeletal muscle satellite cells can be used to study activation in vitro. *Int. J. Biochem. Cell Biol.* **38**(10), 1678–1685. https://doi.org/10.1016/j.biocel.2006.04.003 (2006).
23. Tatsumi, R. et al. Satellite cell activation in stretched skeletal muscle and the role of nitric oxide and hepatocyte growth factor. *Am. J. Physiol. Cell Physiol.* **290**(6), C1487–C1494. https://doi.org/10.1152/ajpcell.00513.2005 (2006).
24. Tatsumi, R. et al. A role for calcium-calmodulin in regulating nitric oxide production during skeletal muscle satellite cell activation. *Am. J. Physiol. Cell Physiol.* **296**(4), C922–C929. https://doi.org/10.1152/ajpcell.00471.2008 (2009).
25. Anderson, J. E. A role for nitric oxide in muscle repair: Nitric oxide-mediated activation of muscle satellite cells. *Mol. Biol. Cell* **11**(5), 1859–1874. https://doi.org/10.1091/mbc.11.5.1859 (2000).
26. Tatsumi, R. & Allen, R. E. Active hepatocyte growth factor is present in skeletal muscle extracellular matrix. *Muscle Nerve* **30**(5), 654–658. https://doi.org/10.1002/mus.20114 (2004).
27. Tatsumi, R. & Allen, R. E. Mechano-biology of resident myogenic stem cells: Molecular mechanism of stretch-induced activation of satellite cells. *Anim. Sci. J.* **79**(3), 279–290. https://doi.org/10.1111/j.1740-0929.2008.00528.x (2008).
28. Yamada, M. et al. Matrix metalloproteinases are involved in mechanical stretch-induced activation of skeletal muscle satellite cells. *Muscle Nerve* **34**(3), 313–319. https://doi.org/10.1002/mus.20601 (2006).
29. Yamada, M. et al. Matrix metalloproteinase-2 mediates stretch-induced activation of skeletal muscle satellite cells in a nitric oxide-dependent manner. *Int. J. Biochem. Cell Biol.* **40**(10), 2183–2191. https://doi.org/10.1016/j.biocel.2008.02.017 (2008).
30. Tatsumi, R. Mechano-biology of skeletal muscle hypertrophy and regeneration: Possible mechanism of stretch-induced activation of resident myogenic stem cells. *Anim. Sci. J.* **81**(1), 11–20. https://doi.org/10.1111/j.1740-0929.2009.00712.x (2010).
31. Hara, M. et al. Calcium influx through a possible coupling of cation channels impacts skeletal muscle satellite cell activation in response to mechanical stretch. *Am J Physiol Cell Physiol* **302**(12), C1741–C1750. https://doi.org/10.1152/ajpcell.00068.2012 (2012).
32. Elgaabari, A. et al. Age-related nitration/dysfunction of myogenic stem cell activator HGF. *Aging Cell* **23**(2), 14041. https://doi.org/10.1111/acel.14041 (2024).
33. Brack, A. S. et al. Increased Wnt signaling during aging alters muscle stem cell fate and increases fibrosis. *Science* **317**(5839), 807–810. https://doi.org/10.1126/science.1144090 (2007).
34. Conboy, I. M. & Rando, T. A. Aging, stem cells and tissue regeneration: Lessons from muscle. *Cell Cycle* **4**(3), 407–410. https://doi.org/10.4161/cc.4.3.1518 (2005).
35. Evans, W. J. & Lexell, J. Human aging, muscle mass, and fiber type composition. *J Gerontol A Biol Sci Med Sci* **50A**(11), 11–16. https://doi.org/10.1093/gerona/50a.special_issue.11 (1995).
36. Korhonen, M. T. et al. Aging, muscle fiber type, and contractile function in sprint-trained athletes. *J. Appl. Physiol.* **101**(3), 906–917. https://doi.org/10.1152/japplphysiol.00299.2006 (2006).
37. Alway, S. E., Myers, M. J. & Mohamed, J. S. Regulation of satellite cell function in sarcopenia. *Front. Aging Neurosci.* **6**, 246. https://doi.org/10.3389/fnagi.2014.00246 (2014).
38. Sousa-Victor, P., García-Prat, L. & Muñoz-Cánoves, P. Control of satellite cell function in muscle regeneration and its disruption in ageing. *Nat. Rev. Mol. Cell Biol.* **23**(3), 204–226. https://doi.org/10.1038/s41580-021-00421-2 (2021).
39. Taylor, J. A. et al. Multisystem physiological perspective of human frailty and its modulation by physical activity. *Physiol Rev* **103**(2), 1137–1191. https://doi.org/10.1152/physrev.00037.2021 (2023).
40. Ischiropoulos, H. Protein tyrosine nitration—an update. *Arch. Biochem. Biophys.* **484**(2), 117–121. https://doi.org/10.1016/j.abb.2008.10.034 (2009).
41. Viner, R. I., Ferrington, D. A., Hühmer, A. F. R., Bigelow, D. J. & Schöneich, C. Accumulation of nitrotyrosine on the SERCA2a isoform of SR Ca-ATPase of rat skeletal muscle during aging: a peroxynitrite-mediated process?. *FEBS Lett* **379**(3), 286–290. https://doi.org/10.1016/0014-5793(95)01530-2 (1996).
42. Fugere, N. A., Ferrington, D. A. & Thompson, L. V. Protein nitration with aging in the rat semimembranosus and soleus muscles. *J Gerontol A Biol Sci Med Sci* **61**(8), 806–812. https://doi.org/10.1093/Gerona/61.8.806 (2006).
43. Pandya, C. D. et al. Age-dependent oxidative stress elevates arginase 1 and uncoupled nitric oxide synthesis in skeletal muscle of aged mice. *Oxid Med Cell Longev* **2019**, 1704650. https://doi.org/10.1155/2019/1704650 (2019).
44. Good, P. F., Hsu, A., Werner, P., Perl, D. P. & Olanow, C. W. Protein nitration in Parkinson's disease. *J Neuropathol Exp Neurol* **57**(4), 338–342. https://doi.org/10.1097/00005072-199804000-00006 (1998).
45. Horiguchi, T. et al. Nitration of tau protein is linked to neurodegeneration in tauopathies. *Am. J. Pathol.* **163**(3), 1021–1031. https://doi.org/10.1016/s0002-9440(10)63462-1 (2003).
46. Reyes, J. F. et al. A possible link between astrocyte activation and tau nitration in Alzheimer's disease. *Neurobiol Dis* **31**(2), 198–208. https://doi.org/10.1016/j.nbd.2008.04.005 (2008).
47. Matsuda, Y. Preventive and therapeutic effects in rats of hepatocyte growth factor infusion on liver fibrosis/cirrhosis. *Hepatology* **26**(1), 81–89. https://doi.org/10.1053/jhep.1997.v26.pm0009214455 (1997).
48. Matsumoto, K., & Nakamura, T. (1998). Plasminogen-related growth factors. *Ciba Found Symp*, 212, pp. 198-214. Wiley Online Library, John Wiley & Sons.

49. Ueki, T. et al. Hepatocyte growth factor gene therapy of liver cirrhosis in rats. *Nat. Med.* **5**(2), 226–230. https://doi.org/10.1038/5593 (1999).
50. Matsumoto, K. Renotropic role and therapeutic potential of HGF in the kidney. *Nephrol. Dial. Transplant.* **17**(suppl. 9), 59–61. https://doi.org/10.1093/ndt/17.suppl_9.59 (2002).
51. Morishita, R. et al. Therapeutic angiogenesis using hepatocyte growth factor (HGF). *Curr. Gene Ther.* **4**(2), 199–206. https://doi.org/10.2174/1566523043346453 (2004).
52. Powell, R. J., Goodney, P., Mendelsohn, F. O., Moen, E. K. & Annex, B. H. Safety and efficacy of patient specific intramuscular injection of HGF plasmid gene therapy on limb perfusion and wound healing in patients with ischemic lower extremity ulceration: Results of the HGF-0205 trial. *J Vasc Surg* **52**(6), 1525–1530. https://doi.org/10.1016/j.jvs.2010.07.044 (2010).
53. Sala, V. & Crepaldi, T. Novel therapy for myocardial infarction: Can HGF/Met be beneficial?. *Cell. Mol. Life Sci.* **68**(10), 1703–1717. https://doi.org/10.1007/s00018-011-0633-6 (2011).
54. Takano, M. et al. Enhanced functional recovery from spinal cord injury in aged mice after stem cell transplantation through HGF induction. *Stem Cell Rep* **8**(3), 509–518. https://doi.org/10.1016/j.stemcr.2017.01.013 (2017).
55. Sanada, F. et al. Therapeutic angiogenesis using HGF plasmid. *Ann. Vasc. Dis.* **13**(2), 109–115. https://doi.org/10.3400/avd.ra.20-00035 (2020).
56. Tanaka, S. et al. In vitro immuno-prevention of nitration/dysfunction of myogenic stem cell activator HGF, towards developing a strategy for age-related muscle atrophy. *Aging Cell* **23**(10), e14337. https://doi.org/10.1111/acel.14337 (2024).
57. Tawarayama, H. et al. Glutathione trisulfide prevents lipopolysaccharide-induced inflammatory gene expression in retinal pigment epithelial cells. *Ocul. Immunol. Inflamm.* **30**(4), 789–800. https://doi.org/10.1080/09273948.2020.1833224 (2020).
58. Tawarayama, H. et al. Glutathione trisulfide prevents lipopolysaccharide-induced retinal inflammation via inhibition of proinflammatory cytokine production in glial cells. *Sci Rep* **13**, 11513. https://doi.org/10.1038/s41598-023-38696-4 (2023).
59. Zhang, T. et al. Enhanced cellular polysulfides negatively regulate TLR4 signaling and mitigate lethal endotoxin shock. *Cell Chem Biol* **26**(5), 686–698. https://doi.org/10.1016/j.chembiol.2019.02.003 (2019).
60. Ida, T. et al. Reactive cysteine persulfides and S-polythiolation regulate oxidative stress and redox signaling. *Proc. Natl. Acad. Sci. U. S. A.* **111**(21), 7606–7611. https://doi.org/10.1073/pnas.1321232111 (2014).
61. Akaike, T. et al. Cysteinyl-tRNA synthetase governs cysteine polysulfidation and mitochondrial bioenergetics. *Nat Commun* **8**(1), 1177 (2017).
62. Elgaabari, A. et al. A pilot study on nitration/dysfunction of NK1 segment of myogenic stem cell activator HGF. *Biochem Biophys Rep* **31**, 101295. https://doi.org/10.1016/j.bbrep.2022.101295 (2022).
63. Allen, R. E., Temm-Grove, C. J., Sheehan, S. M. & Rice, G. Skeletal muscle satellite cell cultures. *Methods Cell Biol* **52**(8), 155–176. https://doi.org/10.1016/s0091-679X(08)60378-7 (1997).
64. Kuwakado, S. et al. Distribution of myogenic stem cell activator, hepatocyte growth factor, in skeletal muscle extracellular matrix and effect of short-term disuse and reloading. *PLoS One* **20**(9), e0321839. https://doi.org/10.1371/journal.pone.0321839 (2025).
65. Yamada, M. et al. High concentrations of HGF inhibit skeletal muscle satellite cell proliferation in vitro by inducing expression of myostatin: A possible mechanism for re-establishing satellite cell quiescence in vivo. *Am. J. Physiol. Cell Physiol.* **298**(3), C465–C476. https://doi.org/10.1152/ajpcell.00449.2009 (2010).
66. Anderson, J. E., Zhu, A. & Mizuno, T. M. Nitric oxide treatment attenuates muscle atrophy during hind limb suspension in mice. *Free Radic. Biol. Med.* **115**, 458–470. https://doi.org/10.1016/j.freeradbiomed.2017.12.021 (2018).
67. Uchikawa, E., Chen, Z., Xiao, G. Y., Zhang, X. & Bai, X. C. Structural basis of the activation of c-MET receptor. *Nat. Commun.* **12**(1), 4074. https://doi.org/10.1038/s41467-021-24367-3 (2021).
68. Chakravarti, B. & Chakravarti, D. N. Protein tyrosine nitration: Role in aging. *Curr. Aging Sci.* **10**(4), 246–262. https://doi.org/10.2174/1874609810666170315112634 (2017).
69. Kanski, J., Hong, S. J. & Schöneich, C. Proteomic analysis of protein nitration in aging skeletal muscle and identification of nitrotyrosine-containing sequences in vivo by nanoelectrospray ionization tandem mass spectrometry. *J. Biol. Chem.* **280**(25), 24261–24266. https://doi.org/10.1074/jbc.M501773200 (2005).
70. Prolo, C., Piacenza, L. & Radi, R. Peroxynitrite: A multifaceted oxidizing and nitrating metabolite. *Curr. Opin. Chem. Biol.* **80**, 102459. https://doi.org/10.1016/j.cbpa.2024.102459 (2024).
71. Mihm, M. J., Coyle, C. M., Schanbacher, B. L., Weinstein, D. M. & Bauer, J. A. Peroxynitrite induced nitration and inactivation of myofibrillar creatine kinase in experimental heart failure. *Cardiovasc Res* **49**(4), 798–807. https://doi.org/10.1016/s0008-6363(00)00307-2 (2001).
72. Shishehbor, M. H. et al. Association of nitrotyrosine levels with cardiovascular disease and modulation by statin therapy. *JAMA* **289**(13), 1675–1680. https://doi.org/10.1001/jama.289.13.1675 (2003).
73. Barreiro, E., Gea, J., Corominas, J. M. & Hussain, S. N. A. Nitric oxide synthases and protein oxidation in the quadriceps femoris of patients with chronic obstructive pulmonary disease. *Am J Resp Cell Mol Biol* **29**(6), 771–778. https://doi.org/10.1165/rcmb.2003-0138oc (2003).
74. Gochman, E., Mahajna, J. & Reznick, A. Z. NF-κB activation by peroxynitrite through IκBα-dependent phosphorylation versus nitration in colon cancer cells. *Anticancer Res* **31**(5), 1607–1617 (2011).
75. Markowitz, J. et al. Nitric oxide mediated inhibition of antigen presentation from DCs to CD4$^+$ T cells in cancer and measurement of STAT1 nitration. *Sci Rep* **7**, 15424. https://doi.org/10.1038/s41598-017-14970-0 (2017).
76. Zhan, X., Huang, Y. & Qian, S. Protein tyrosine nitration in lung cancer: Current research status and future perspectives. *Curr. Med. Chem.* **25**(29), 3435–3454. https://doi.org/10.2174/0929867325666180221140745 (2018).
77. Castegna, A. et al. Proteomic identification of nitrated proteins in Alzheimer's disease brain. *J. Neurochem.* **85**(6), 1394–1401. https://doi.org/10.1046/j.1471-4159.2003.01786.x (2003).
78. He, Y., Yu, Z. & Chen, S. Alpha-synuclein nitration and its implications in Parkinson's disease. *ACS Chem Neurosic* **10**(2), 777–782. https://doi.org/10.1021/acschemneuro.8b00288 (2019).

Acknowledgements

The helpful discussions and advice on trisulfides with/from Dr. Etsuo Ohshima (Kyowa Pharma Chemical Co., Ltd., Toyama, Japan) were invaluable. Special thanks to Ms. Akiko Sato (Kyushu University, Japan) for technical assistance concerning animal care and satellite-cell culture experiments. Many thanks to Mr. Hiroyuki Ueki (KEYENCE, Osaka, Japan) for the technical guidance and assistance on immunofluorescence microscopy. The authors thank the Center for Advanced Equipment and Educational Support, Faculty of Agriculture, Kyushu University for the use of the ECL-detection imaging system and the plate-reader. Trisulfides, GSSSG and LASSS, were provided from Kyowa Pharma Chemical Co., Ltd. (Toyama, Japan). The anti-BrdU antibody (G3G4) developed by Dr. S. J. Kaufman and the anti-desmin antibody (D3) developed by Dr. D. A. Fischman were obtained from the Developmental Studies Hybridoma Bank developed under the auspices of the NICHD and maintained by The University of Iowa, Department of Biological Sciences, Iowa City, IA 52242, Iowa.

Author contributions

R.T. conceived the project. K.Z., M.S., R.T. designed the experiments. K.Z., M.S., R.M., K.S., A.E., S.T., J.M., K.M., R.F., J.H., T.N., R.T. performed the experiments. T.N. worked on the 3D model of the HGF-NK2 region accessible to lipoic acid trisulfide and its graphical representation. K.Z., M.S., R.M., K.S., A.E., S.T., J.M., K.M., R.F., J.H., T.N., J.E.A., R.T. analyzed the data. S.S., W.M., T.M., I.Y., T.S. contributed reagents, materials, and/or analysis tools and provided advice on project progress and technical help. K.Z., R.T. wrote original draft and J.E.A., R.T. reviewed and edited the manuscript.

Funding

The research was supported in part by Grants-in-Aid for Challenging Exploratory Research and Scientific Research (B) from the Japan Society for the Promotion of Science (JSPS KAKENHI Grant Numbers JP26660218, JP21H02347, and JP24K01911, respectively) and by grant funds from the Uehara Memorial Foundation and Ito Foundation (all to R. Tatsumi). Dr. Alaa Elgaabari was supported by a JSPS Postdoctoral Fellowship for Research in Japan (Standard FY 2022; P22389) during the course of this research. The funders had no role in study design, data collection and analysis, decision to publish, or preparation of the manuscript, and did not provide support in the form of salaries for any authors.

Declarations

Competing interests

The authors declare no competing interests.

Additional information

Supplementary Information The online version contains supplementary material available at https://doi.org/10.1038/s41598-026-60835-w.

Correspondence and requests for materials should be addressed to R.T.

Reprints and permissions information is available at www.nature.com/reprints.

Publisher's note Springer Nature remains neutral with regard to jurisdictional claims in published maps and institutional affiliations.